

PULSATIONS OF THE SX PHE STAR BL CAMELOPARDALIS

PENG. ZONG,^{1,2} ALI. ESAMDIN,^{1,2} JIAN NING. FU,³ HU BIAO. NIU,^{1,3} GUO JIE. FENG,^{1,2} TAO ZHI. YANG,¹
CHUN HAI. BAI,¹ YU. ZHANG,¹ AND JIN ZHONG. LIU¹

¹*Xinjiang Astronomical Observatory, Chinese Academy of Sciences, Urumqi, Xinjiang 830011, People's Republic of China*

²*University of Chinese Academy of Sciences, Beijing 100049, People's Republic of China*

³*Department of Astronomy, Beijing Normal University, Beijing 100875, People's Republic of China*

Submitted to PASP

ABSTRACT

We carried out photometric observations of the SX Phe star BL Cam in 2014, 2017 and 2018 using Nanshan 1-m telescope. In addition to the dominated frequency of $25.5790(3) \text{ cd}^{-1}$ and its two harmonics, an independent frequency of $25.247(2) \text{ cd}^{-1}$, which is a nonradial mode frequency, was detected from the data in 2014. A total of 123 new times of light maxima were determined from our light curves in the three years, which, together with that published in the literature, were used to analyze the $O-C$ diagram. The change rate of the main period was derived as $(1/P)(dP/dt) = -2.39(8) \times 10^{-8} \text{ yr}^{-1}$, which is lower than that published in previous literature. A periodical change with a period of 14.01(9) yr was found in the residuals of the $O-C$ curve fitting. If it was caused by the light-time effect, BL Cam should be a binary system. The mass of the companion was restricted as low as that of a brown dwarf. No evidence of the triple system suggested by previous authors was shown in our analysis.

Keywords: stars: variables: delta Sct—stars: individual: BL Cam—stars: oscillations—techniques: photometric

1. INTRODUCTION

SX Phe stars are high-amplitude δ Scuti variables (HADS) belonging to Population II stars with high spatial motion and low metallicity (Fauvaud et al. 2006). However, some of them are metal-rich and more like halo A-type stars found in the *Kepler* field of view (Nemec et al. 2017). The SX Phe stars have masses of $\sim 1.0 - 1.2 M_{\odot}$ and relatively young ages $\sim 2.0 - 5.0$ Gyr (Nemec & Mateo 1990). They are mostly located in the blue stragglers of globular clusters (Martinazzi et al. 2015; Kains et al. 2015; Kopacki 2013) while some of them are also found in the field. However, there are no observation differences in the physical properties of SX Phe stars in the field and in the globular clusters (McNamara 2011). The pulsating behavior of the SX Phe stars in the field is similar to the Population I high amplitude δ Scuti stars (Catelan & Smith 2015). Most SX Phe stars have short periods ($\lesssim 0.08$ d) and large amplitudes (> 0.3 mag) (Fauvaud et al. 2006). It is generally assumed that the metal-poor HADS show only two radial pulsation modes, but BL Cam ($\alpha_{2000} = 03^h47^{min}19^s$, $\delta_{2000} = +63^{\circ}22'07''$, $\langle V \rangle \sim 13.1$ mag, $\Delta V \sim 0.33$ mag, Rodríguez & Breger 2001) as a SX Phe star in the field seems to be an exception (McNamara 2011).

BL Cam was discovered by Giclas et al. (1970) and considered as a possible candidate of white dwarf. Berg & Duthie (1977) noted that it is a pulsating star with the period of 0.039 days and the amplitude of 0.33 mag. McNamara (1997) determined its metal abundance of $[\text{Fe}/\text{H}] = -2.4$ and classified it as a Population II star. Its multiperiodic nature has been studied by previous authors (Fauvaud et al. 2006; Rodríguez et al. 2007; Fu et al. 2008). Hintz et al. (1997) reported its first overtone of 32.679 cd^{-1} , and the period ratio of the first overtone to the fundamental mode of 0.783. The first overtone around 31.6 cd^{-1} was also detected by previous authors (Zhou et al. 1999; Kim & Sim 1999; Zhou et al. 2001; Wolf et al. 2002), leading to the period ratio of 0.810. However, the first overtone was not detected by Fu et al. (2008). Rodríguez et al. (2007) carried out a multi-site photometric campaign of BL Cam and detected 21 independent pulsation frequencies (excluding the fundamental mode) with amplitudes ranging from 1.6 to 7.4 mmag. The first overtone and the period ratio they obtained are the same with that of Hintz et al. (1997). The multiperiodic nature of BL Cam and the controversies of its first overtone make it deserve further study.

Hintz et al. (1997) discovered the long-term increase of the main period using the $O-C$ method. Breger & Pamyatnykh (1998) performed an analysis

of the $O-C$ diagram, revealing an increase of 0.02 s of the main period over the past 20 years with the period variation rate of $(1/P)(dP/dt) = 2.90 \times 10^{-7} \text{ yr}^{-1}$. Kim et al. (2003) pointed out a reversal trend in the $O-C$ diagram of BL Cam since 1999, which led to a possible sinusoidal behavior, suggesting that BL Cam might be a binary system. The binary system analysis of $O-C$ diagram of BL Cam has been published in previous literature (Fauvaud et al. 2006; Fu et al. 2008). Fauvaud et al. (2010) performed a triple system analysis of the $O-C$ diagram. However, the determination of the second companion's parameters was not successful. Conidis & Delaney (2013) suggested that there might be an abrupt change in the main period, probably because BL Cam is a triple system.

To study the characteristics of pulsation and behaviors of the main period of BL Cam, CCD photometric observations had been performed in 2014, 2017, and 2018. Section 2 of this paper presents observations and data reduction. Sections 3 and 4 give the results of frequency analysis and the $O-C$ diagram diagnosis, respectively. We discuss our results in Section 5. The summary of this work is given in Section 6.

2. OBSERVATIONS AND DATA REDUCTION

BL Cam was observed using the 1-m Nanshan Optical Wide-field Telescope (NOWT) of Xinjiang Astronomical Observatory (XAO) in 2014, 2017, and 2018. The location of NOWT is 87.1° E and 43.8° N, near Urumqi of Xinjiang in China. The telescope was equipped with a standard Johnson multicolor filter system (i.e., U B V R I filters) (e.g. Cousins 1976) and an E2V CCD 203-82 (blue) camera mounted on the primary focus of the telescope. The CCD camera, which has $4\text{K} \times 4\text{K}$ pixels and a $1.3^{\circ} \times 1.3^{\circ}$ field of view, operated at a temperature of about -120°C cooling with liquid nitrogen (Song et al. 2016; Ma et al. 2018).

The exposure time of observations was either 3 s or 5 s in 2014, 10 s in 2017, and 12 s in 2018. The exposure time increased in different observation seasons in order to get a high signal-to-noise ratio (S/N). A total of 11,854 CCD images are obtained on 14 nights using V filter, including 6831 images on nine nights in 2014, 4173 images on four nights in 2017 and 850 images on one night in 2018. The journal of observations of BL Cam is given in Table 1.

The IRAF¹ (Tody 1986, 1993) package was used to reduce all CCD images by subtracting the bias and making

¹ Image Reduction and Analysis Facility is developed and distributed by the National Optical Astronomy Observatories, which is operated by the Association of Universities for Research in As-

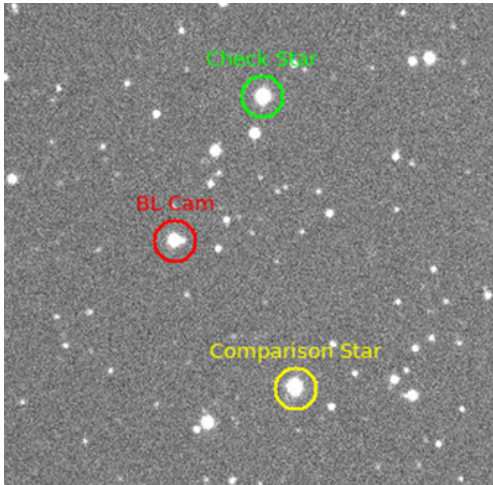


Figure 1. Trimmed CCD image of BL Cam collected by NOWT. BL Cam, the comparison and the check star are marked with red, yellow, and green circles, respectively.

flat field correction using the master flat. The dark correction was not considered because the thermal noise of the CCD camera was negligible with the value less than $1 \text{ e pix}^{-1} \text{ h}^{-1}$ at the temperature of -120°C (Yang et al. 2018).

Two stars selected by Conidis & Delaney (2013) were taken as the comparison and the check star, respectively, as shown in Figure 1. The standard deviations of the differential magnitudes between the check star and the comparison star yield the estimations of the photometric precisions, with typical values of $0^m.005$ and $0^m.035$ in good and poor observational conditions, respectively. The light curves of BL Cam were obtained by calculating the differential magnitudes between the target and the comparison star. For frequency determination, every data point of the light curve takes its own weighting, which is the inverse square of the photometric precision. Figure 2 shows the light curves of BL Cam in V band in 2014, 2017 and 2018, respectively.

3. FREQUENCY ANALYSIS

Frequency analysis was performed with the light curves in 2014 by using Period04 (Lenz & Breger 2005), which focuses on multi-frequency analysis using Fourier transform and least-square fitting. The following formula was applied to the fitting of the light curves:

$$m = m_0 + \sum A_i \sin[2\pi(f_i t + \varphi_i)] \quad (1)$$

tromy under operative agreement with the National Science Foundation.

where A_i , f_i and φ_i are the amplitude, frequency, and phase, respectively. We follow a standard pre-whitening procedure.

First, the highest peak in the spectrum of the light curves was selected as a significant frequency, which was taken to do least-square fitting to determine the values of frequency, amplitude, and phase. Theoretical light curves were then constructed with the solution of the determined frequency and subtracted from the origin light curves to get the residual light curves. Then, we picked out the highest peak in the spectrum of the residual light curve as the next significant frequency and subtracted the light curves constructed with the solutions of all the detected frequencies from the origin light curves. We repeated the above steps until no significant frequency was detected. We adopted $S/N > 6$ (Baran et al. 2015; Barceló Forteza et al. 2015) as the criterion of resolving the frequencies. Table 2 lists the significant frequencies detected from the light curves in 2014.

The dominated frequency $f_0 = 25.57827(9) \text{ cd}^{-1}$ and its two harmonics f_1 ($2f_0$), f_4 ($3f_0$) were detected from the light curves in 2014. In Table 2, the frequency detected in the region of $0-3 \text{ cd}^{-1}$ was not considered to be significant frequencies of the variable star, as it may very possibly be caused by either the instrument sensitivity instability or variations of the atmospheric transparency as suggested by Yang et al. (2012) and Yang et al. (2018). The frequency of f_3 , which is not linked in any way with the other significant frequencies, is considered as an independent frequency. Figures 3 and 4 show the spectral window and Fourier power spectra of frequency pre-whitening process for the light curves of BL Cam in 2014, respectively.

Because the data collected in 2017 and 2018 covered only four nights and one night respectively, we did not try to do frequency analysis with the data in these two years.

4. PERIOD VARIATION ANALYSIS

4.1. Times of maximum light

The $O-C$ method is a classical method for studying the periodic variations of the variable star as it is sensitive to the cumulative effect of periodic changes (Sterken 2005; Dejaiffe 2007). The times of maximum light of BL Cam were derived by fitting a third or fourth order polynomial around each peak of the light curves, the median uncertainty is $\sigma = 0.0001 \text{ d}$. In total, 123 new times of light maxima were determined and listed in Table 3. Together with the 1460 times of light maxima published in the previous literature (Berg & Duthie 1977; McNamara & Feltz 1978; Rodriguez et al. 1990; Hintz et al. 1997; Zhou et al. 1999; Blake et al. 2000;

Table 1. Journal of observations for BL Cam in 2014, 2017 and 2018.

Date	Exposure Time (second)	Filter	CCD Images	Length of Observation (hour)
2014.10.25	3	V	713	8.7
2014.10.26	3	V	854	10.4
2014.10.29	3	V	707	8.6
2014.10.31	3	V	788	9.6
2014.11.01	5	V	876	10.7
2014.11.02	5	V	846	10.3
2014.11.03	5	V	874	10.6
2014.11.05	5	V	564	6.9
2014.11.06	5	V	609	7.4
2017.09.04	10	V	216	2.6
2017.10.30	10	V	1007	6.5
2017.11.02	10	V	1089	7.0
2017.11.03	10	V	1861	12.0
2018.10.21	12	V	850	6.0
total			11854	117.3

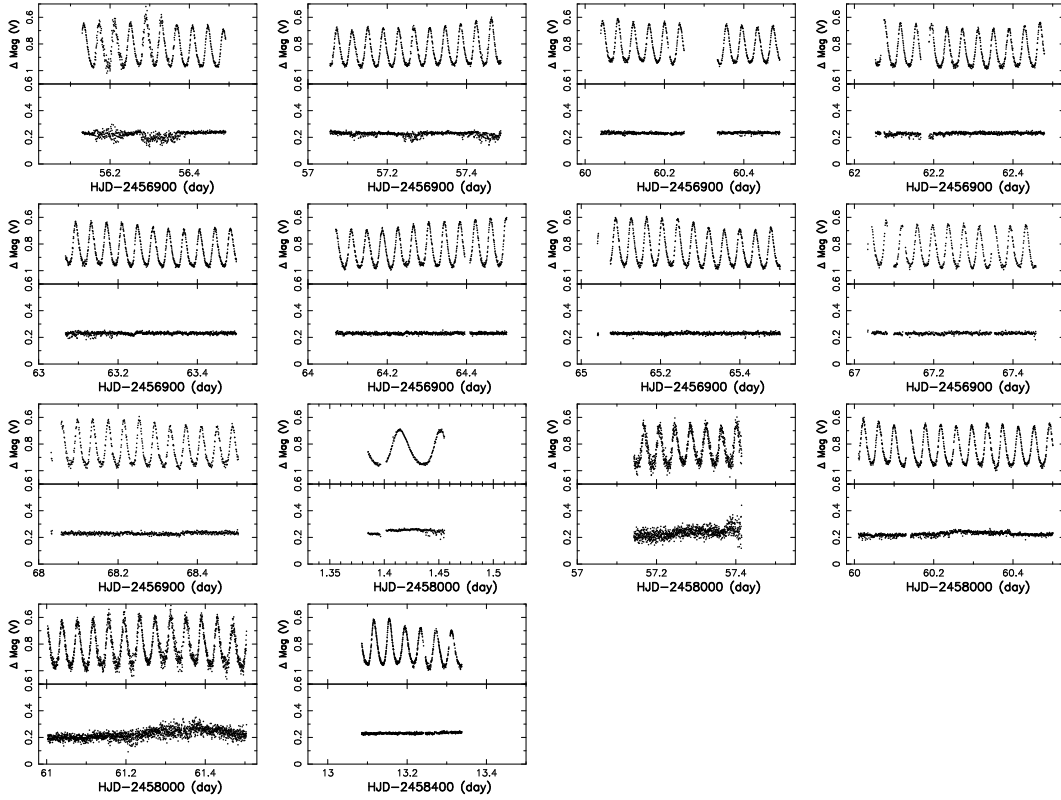
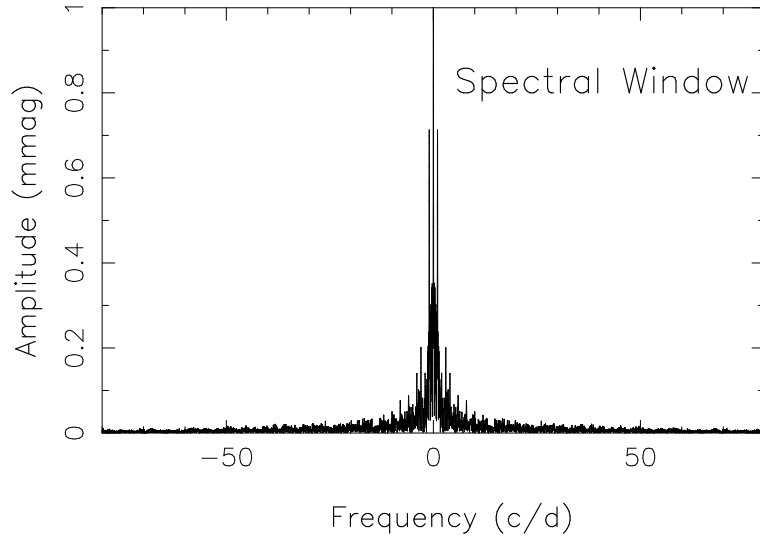
**Figure 2.** Light curves of BL Cam in V band in 2014, 2017, and 2018. The top panel in each subfigure show the magnitude difference between BL Cam and the comparison star, while the bottom panels present the magnitude difference between the check star and the comparison star.

Table 2. Frequencies Detected from the Light Curves in 2014.

ID	Freq. (cd^{-1})	Ampl. (mmag)	S/N	Identification
f_0	25.57827 (9)	148 (1)	141.0	Main frequency
f_1	51.1566 (4)	33.3 (7)	46.0	$2f_0$
f_2	1.5840 (7)	17.0 (2)	7.2	Alias
f_3	25.247 (2)	8.0 (1)	7.5	Nonradial
f_4	76.731 (2)	5.7 (4)	16.1	$3f_0$

**Figure 3.** Spectral window of the light curves of BL Cam in V band in 2014.

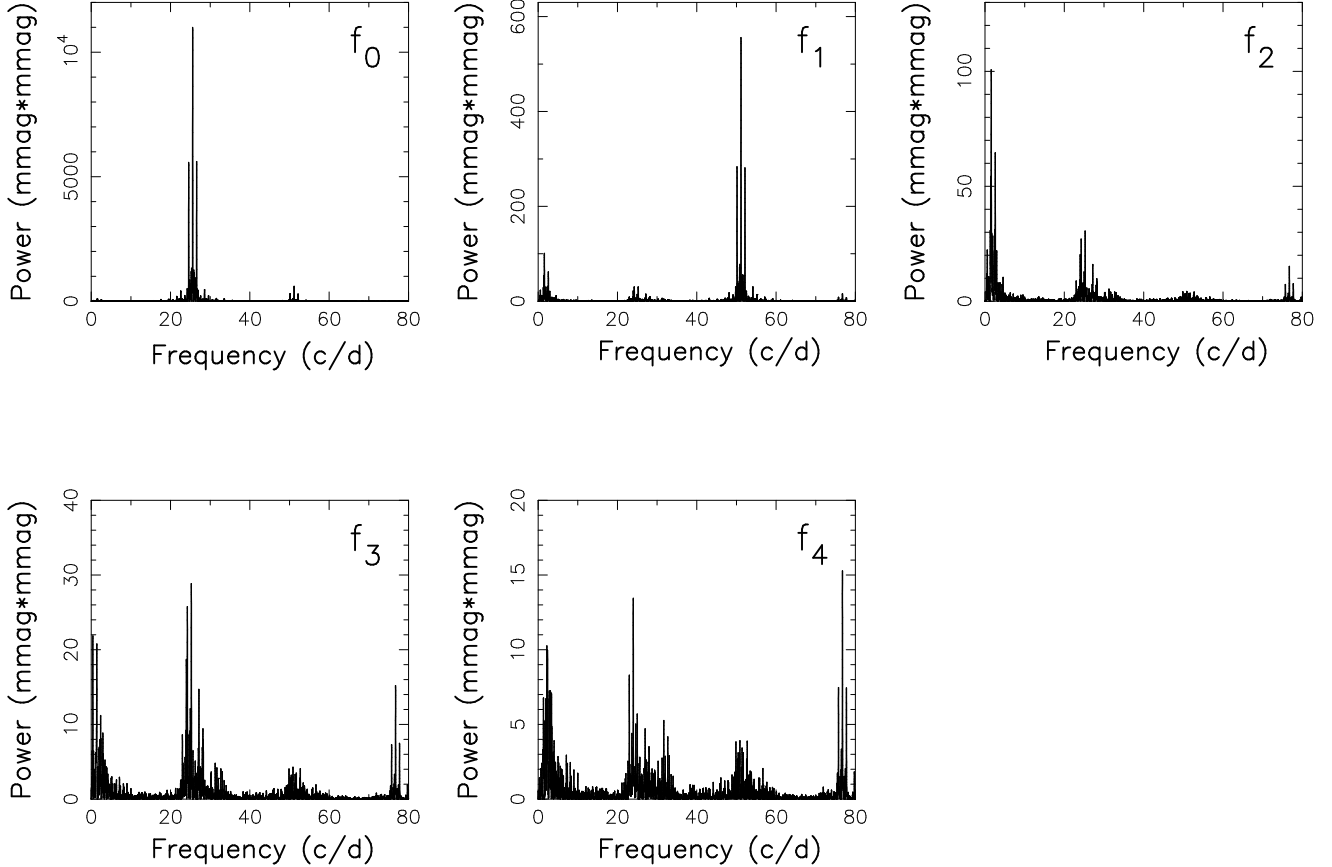


Figure 4. Fourier power spectra of the frequency pre-whitening process for the light curves of BL Cam in V band in 2014.

van Cauteren & Wils 2000; Zhou et al. 2001; Wolf et al. 2002; Kim et al. 2003; Fauvaud et al. 2006; Fu et al. 2008; Fauvaud et al. 2010; Conidis & Delaney 2013), we tried to reanalyze the $O-C$ diagram of BL Cam.

4.2. $O-C$ diagram

Using the 1583 times of the light maxima and the linear ephemeris given by Zhou et al. (1999):

$$HJD = 2443125.8015 + 0.03909785E, \quad (2)$$

the number of cycle (E) for each observed maximum is calculated. Linear fitting of Heliocentric Julian Day (HJD) and cycle number (E) yields a new period value of 0.0390979135 (9) and a new linear ephemeris as

$$HJD = 2443125.7938(4) + 0.0390979135(9)E, \quad (3)$$

Using the new linear ephemeris (Equation 3), the values of $O-C$ could be determined. The times of light maxima determined in this work, the numbers of cycle (E) and the values of $O-C$ are listed in Table 3. Conidis & Delaney (2013) show that a discontinues change in the main period is supported by the whole data of $O-C$ diagram. In this paper, we do not intend to explore the discontinue change of the main period,

which was discussed by them. Fu et al. (2008) carried out the binary analysis for the $O-C$ diagram on the data of $HJD > 2448800$ ($E > 150000$). We do the fitting to the data of $E > 150000$ to determine whether BL Cam is in a binary system. To determine the change rate of the main period $(1/P)(dP/dt)$, a parabolic fit is performed for the $O-C$ diagram. Our fit is concentrated on the data with $E > 150000$, which leads to a new quadratic ephemeris:

$$O-C = -2.00(7) \times 10^{-13} \times E^2 + 1.25(4) \times 10^{-7} \times E - 0.0190(5), \quad (4)$$

The standard deviation σ of the residuals of the quadratic fitting is 0.0015 days. The corresponding period change rate is $(1/P)(dP/dt) = -2.39(8) \times 10^{-8} \text{ yr}^{-1}$.

When the parabolic curve (as shown in the top panel of Figure 5) is subtracted from the $O-C$ diagram, the residuals show a significant periodic change (as shown in the bottom panel of Figure 5), which might be caused by the light-time effect. The periodic variation of the residuals could be interpreted with a binary system hypothesis and plotted in Figure 6. The $O-C$ residuals were fitted with the following formula (Borkovits & Hegedues

Table 3. Times of Light Maxima of BL Cam.

Maxima	Cycle	$O-C$	Maxima	Cycle	$O-C$
HJD	E	day	HJD	E	day
2456956.13366	353736	0.00033	2456965.20376	353968	-0.00029
2456956.17328	353737	0.00085	2456965.24336	353969	0.00022
2456956.21215	353738	0.00062	2456965.32123	353971	-0.00011
2456956.25144	353739	0.00082	2456965.36053	353972	0.00009
2456956.29045	353740	0.00073	2456965.39965	353973	0.00011
2456956.33207	353741	0.00325	2456965.43940	353974	0.00077
2456956.36826	353742	0.00034	2456965.47771	353975	-0.00002
2456956.40786	353743	0.00084	2456967.15864	354018	-0.00030
2456956.44660	353744	0.00049	2456967.19770	354019	-0.00034
2456956.48530	353745	0.00009	2456967.23619	354020	-0.00095
2456957.07249	353760	0.00081	2456967.27583	354021	-0.00041
2456957.11114	353761	0.00036	2456967.31501	354022	-0.00032
2456957.15075	353762	0.00087	2456967.39259	354024	-0.00094
2456957.18986	353763	0.00089	2456967.43215	354025	-0.00048
2456957.22806	353764	-0.00001	2456967.47089	354026	-0.00083
2456957.26659	353765	-0.00058	2456968.09761	354042	0.00032
2456957.30750	353766	0.00123	2456968.13594	354043	-0.00045
2456957.34717	353767	0.00180	2456968.17561	354044	0.00012
2456957.38516	353768	0.00070	2456968.21462	354045	0.00003
2456957.42406	353769	0.00050	2456968.25295	354046	-0.00073
2456957.46288	353770	0.00022	2456968.29210	354047	-0.00068
2456960.04380	353836	0.00068	2456968.33114	354048	-0.00074
2456960.08201	353837	-0.00021	2456968.37107	354049	0.00009
2456960.12129	353838	-0.00003	2456968.41068	354050	0.00061
2456960.16170	353839	0.00129	2456968.44969	354051	0.00052
2456960.19956	353840	0.00005	2456968.48851	354052	0.00024
2456960.23783	353841	-0.00078	2458001.41417	380471	-0.00188
2456960.35630	353844	0.00040	2458001.45229	380472	-0.00286
2456960.39474	353845	-0.00026	2458057.16948	381897	-0.00019
2456960.43451	353846	0.00041	2458057.20663	381898	-0.00214
2456960.47344	353847	0.00024	2458057.24689	381899	-0.00098

1996):

$$(O - C)_1 = a_0 + \sum_{i=1}^2 [a_i \cos(i\omega E) + b_i \sin(i\omega E)], \quad (5)$$

The solutions of Equation (5) are listed in Table 4.

5. DISCUSSION

5.1. Additional frequencies in the region of 25-26 cd^{-1}

From Table 2, one notes that in addition to the main frequency f_0 and its two harmonics, one frequency in the 0-3 cd^{-1} region, there is an additional frequency $f_3 = 25.247$ (2) cd^{-1} which has no numerical relation with the above frequencies. Hence, we think it is an independent frequency. As its value is very close to that of the main frequency f_0 , which should be a radial mode due to its high amplitude, f_3 should be a nonradial mode. We should note that the frequencies

2456962.11588	353889	0.00057	2458057.28520	381900	-0.00177
2456962.15526	353890	0.00085	2458057.32509	381901	-0.00097
2456962.23310	353892	0.00050	2458057.36264	381902	-0.00252
2456962.27196	353893	0.00026	2458057.40222	381903	-0.00204
2456962.31194	353894	0.00114	2458060.02277	381970	-0.00105
2456962.35191	353895	0.00201	2458060.09999	381972	-0.00203
2456962.39092	353896	0.00192	2458060.17873	381974	-0.00148
2456962.42940	353897	0.00131	2458060.21731	381975	-0.00200
2456962.46797	353898	0.00078	2458060.25886	381976	0.00045
2456963.09316	353914	0.00040	2458060.29577	381977	-0.00173
2456963.13264	353915	0.00078	2458060.33383	381978	-0.00277
2456963.17104	353916	0.00009	2458060.37357	381979	-0.00213
2456963.20961	353917	-0.00044	2458060.41272	381980	-0.00208
2456963.24855	353918	-0.00060	2458060.45320	381981	-0.00070
2456963.32673	353920	-0.00062	2458061.03836	381996	-0.00201
2456963.36631	353921	-0.00013	2458061.07681	381997	-0.00265
2456963.40563	353922	0.00009	2458061.11725	381998	-0.00131
2456963.44405	353923	-0.00059	2458061.15632	381999	-0.00134
2456963.48333	353924	-0.00041	2458061.19537	382000	-0.00139
2456964.10916	353940	-0.00014	2458061.23450	382001	-0.00135
2456964.14821	353941	-0.00019	2458061.27388	382002	-0.00107
2456964.18739	353942	-0.00011	2458061.31669	382003	0.00264
2456964.22727	353943	0.00067	2458061.39057	382005	-0.00168
2456964.30498	353945	0.00019	2458061.47106	382007	0.00062
2456964.34423	353946	0.00034	2458413.11605	391001	-0.00103
2456964.38365	353947	0.00066	2458413.15456	391002	-0.00161
2456964.42206	353948	-0.00003	2458413.19435	391003	-0.00092
2456964.46020	353949	-0.00099	2458413.23428	391004	-0.00009
2456965.08672	353965	-0.00003	2458413.27298	391005	-0.00049
2456965.12622	353966	0.00037	2458413.31186	391006	-0.00071
2456965.16517	353967	0.00022			

Table 4. The Solutions of Equation (5).

Coefficient	Value	Error(σ)
a_0	1.1×10^{-4}	3.0×10^{-5}
a_1	-9.19×10^{-4}	7.0×10^{-6}
b_1	7.8×10^{-4}	8.0×10^{-5}
a_2	4.6×10^{-4}	4.0×10^{-5}
b_2	1.5×10^{-4}	8.0×10^{-5}
ω	4.8×10^{-5}	3.0×10^{-5}

in the region of 31.6-32.6 cd^{-1} detected by previous

authors (Hintz et al. 1997; Zhou et al. 1999; Kim et al. 2003; Fauvaud et al. 2006; Rodríguez et al. 2007) were not detected in this work. Fu et al. (2008) suggested that this might be due to the amplitude changes, leading the amplitude lower than the photometric limit of the observations.

Hence, we collect all the additional frequencies in the region of 25-26 cd^{-1} of BL Cam in the literature (Zhou et al. 1999, 2001; Fu et al. 2008; Rodríguez et al. 2007) as listed in Table 5. One may find that the number of the frequency, the frequency values and the amplitudes are all different to each other. On the other hand, we see only one additional frequency in the 25-

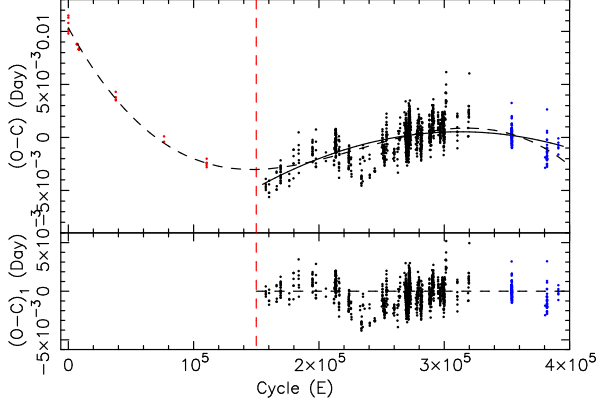


Figure 5. The $O-C$ diagram of BL Cam. The top panel shows the $O-C$ of BL Cam fitted by a quadratic ephemeris for those points in the region of $E > 150000$, and the bottom panel shows the residuals of the quadratic fit. The blue dots are the values of $O-C$ we determined from the light curves in 2014, 2017, and 2018. The red solid dots are in the region of $E < 150000$. The dotted line is the dividing line at $E = 150000$. The black dotted line is the cubic fitting for the data of $O-C$ diagram.

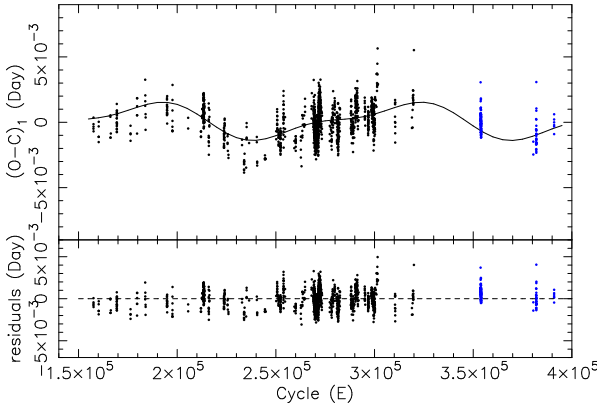


Figure 6. Residuals of the parabolic fit of the $O-C$ curve. The top panel shows the residuals of $O-C$ fitted by Equation (5) (solid line), and the bottom panel shows the residuals after subtracting solutions of Equation (5).

26 cd^{-1} region in the bottom 4 panels of Figure 7. No interpretations are present to these detections.

5.2. Period Changes

The change rate of the main period of BL Cam was determined by previous authors using a parabolic fit (Hintz et al. 1997; Zhou et al. 1999; Fauvaud et al. 2006; Fu et al. 2008; Fauvaud et al. 2010; Conidis & Delaney 2013). The change rate of the main period determined in this work is $(1/P)(dP/dt) = -2.39(8) \times 10^{-8} \text{ yr}^{-1}$. A binary system analysis on the residuals of the $O-C$ is performed in this work. The following parameters of the companion: eccentricity (e'), orbital period (P'), projection of the orbit radius ($A' \sin i'$), and argument

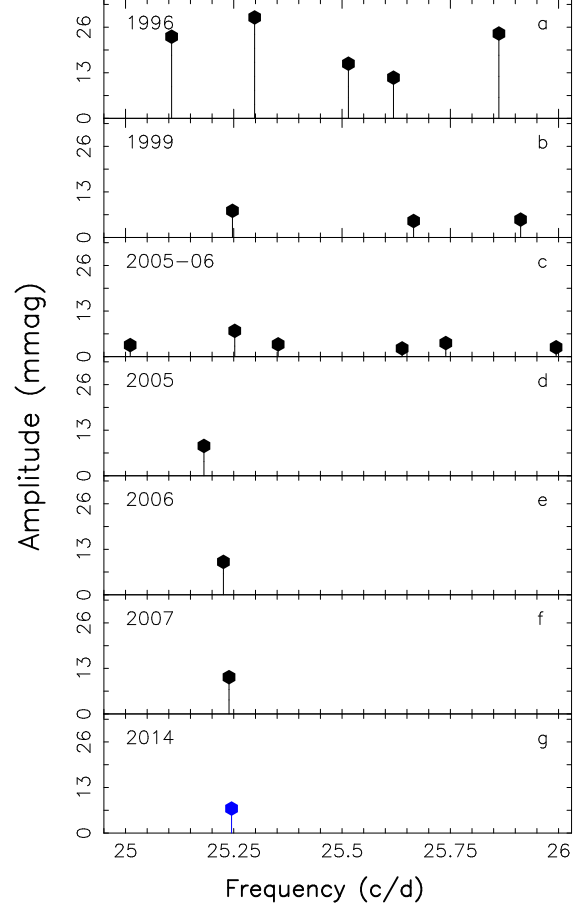


Figure 7. The frequencies detected in the region of $25-26 \text{ cd}^{-1}$ in different years. a)Zhou et al. (1999), b)Zhou et al. (2001), c) Fu et al. (2008), d)Rodríguez et al. (2007), e,f)Fu et al. (2008) and g) this work.

of periastron (ω') listed in Table 6 are determined with the formula adopted by Borkovits & Hegedues (1996). The values of these parameters obtained in this work are consistent with those given by the previous authors (Fauvaud et al. 2006; Fu et al. 2008) except the orbital period and the argument of periastron, which is probably because the newly determined data change the trend of residuals of the $O-C$ fit.

Fu et al. (2008) suggested that the main period of BL Cam might be undergone an abrupt change, because they divided the $O-C$ data into two parts. A triple system analysis for BL Cam was performed by Fauvaud et al. (2010), but determining the orbital parameters of the second companion was unsuccessful. They pointed out that those significant change in $O-C$ might be due to abrupt change of the main period. Conidis & Delaney (2013) obtained the value of the abrupt change of the main period $\Delta P = -0.126(4) \text{ s}$ by dividing $O-C$ data into two parts, i.e. the oldest data of $E < 150000$ and the data in the region of $E >$

Table 5. Frequencies detected in the region of 25-26 cd^{-1} from Different Observation Data Sets.

Year	Freq. (cd^{-1})	Ampl. (mmag)	Reference
	25.2982	28.8	
	25.8622	24.2	
1996	25.1065	23.3	Zhou et al.(1999)
	25.5147	15.6	
	25.6188	11.6	
	25.2469	7.6	
1999	25.9122	5.1	Zhou et al.(2001)
	25.6653	4.7	
	25.25226	7.35	
	25.63866	2.33	
2005-06	25.73943	3.86	Rodríguez et al.(2007)
	25.01079	3.27	
	25.35245	3.48	
	25.99419	2.64	
2005	25.181	8.5	
2006	25.226	9.4	Fu et al.(2008)
2007	25.239	10.5	
2014	25.247(2)	8(1)	this work

150000. They suggested that the abrupt change of the main period might be caused by a third body. They also pointed out that a cubic more appropriately fits the behavior of the $O-C$ diagram as shown in top panel of Figure 5. But the physical meaning of the third order term is not understood. Sterken (2005) suggested that statistical validity must be considered very carefully in studying sudden changes of period. Figure 5 shows the whole fitting of the $O-C$ diagram. The data are not sufficient to prove that the abrupt change of the main period was caused by the third object, and its orbital properties are dependent on the long-term correction of the $O-C$ trend, which need to be confirmed by future observations.

To determine the mass of the companion, we use the mass function adopted in previous literature (Fu et al. 2008; Li & Qian 2010). The value of mass function of the companion is derived to be $1.65(3) \times 10^{-4}$ and it is 17% of that obtained by Fu et al. (2008). This might be due to the orbital period we determined in this work

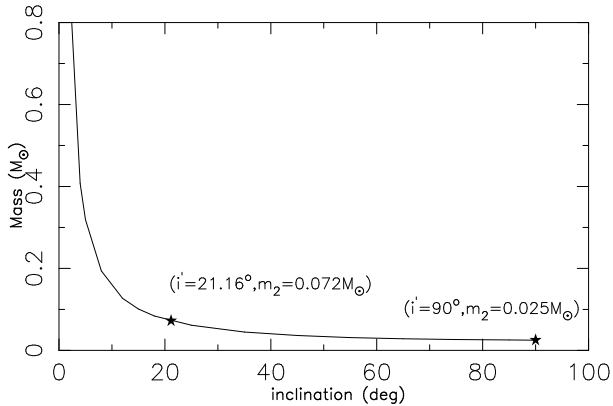
is different from theirs. During the observations of BL Cam we did not detect any eclipsing, hence the inclination of the system can not be precisely determined. Based on the mass of $0.99 M_{\odot}$ of BL Cam determined by McNamara (1997) and the value of mass function given in this work, a relationship between the mass of the companion and the orbital inclination of binary, as shown in Figure 8, could be determined. When the orbital inclination ranges from 21.16° to 90° , the mass of companion is between $0.072 M_{\odot}$ and $0.025 M_{\odot}$. If the inclination distributes randomly, the possibility that the companion is a brown dwarf is 76%.

6. SUMMARY

Based on new photometric observations of BL Cam in 2014, we analyzed its pulsation characteristics. An independent frequency of $25.247(2) \text{cd}^{-1}$ was detected in the region of 25-26 cd^{-1} from the data of 2014. Using newly determined 123 times of light maxima and those published in the previous literature, the $O-C$ analysis

Table 6. Parameters of the Companion Star of BL Cam.

Parameter	Value	Error(σ)
e'	0.80	(7)
ω' (deg)	81.29	(11)
$A' \sin i'$ (AU)	0.210	(8)
P' (yr)	14.01	(9)

**Figure 8.** Inclination versus mass of the second body. The mass of the companion between the two pentagrams corresponds to the mass of brown dwarf.

for BL Cam reveals a period of 0.0390979135 (9) days and an update period change rate of the main period $(1/P)(dP/dt) = -2.39(8) \times 10^{-8} \text{yr}^{-1}$. The residuals of fitting the $O-C$ curve implies that BL Cam might be a binary system in an eccentric orbit with a period of 14.01 (9) yr. The companion might be a brown dwarf. More photometric and spectroscopic observations are needed to reveal the pulsational characteristics and confirm the binary hypothesis of BL Cam.

This research is supported by Nanshan 1 m telescope of Xinjiang Astronomical Observatory, light in China's Western Region: 2015-XBQN-A-02, XBBS-2014-25; National Natural of Science Fundation of China: 11873081, 11673003, 11833002, 11661161016; 2017 Heaven Lake Hundred-Talent Program of Xinjiang Uygur Autonomous Region of China.

Software: Period04 (Lenz & Breger 2005), IRAF (Tody 1986, 1993)

REFERENCES

- Baran, A. S., Koen, C., & Pokrzywka, B. 2015, MNRAS, 448, L16
- Barceló Forteza, S., Michel, E., Roca Cortés, T., & García, R. A. 2015, A&A, 579, A133
- Berg, R. A., & Duthie, J. G. 1977, ApJL, 215, L25
- Blake, R. M., Khosravani, H., & Delaney, P. A. 2000, JRASC, 94, 124
- Breger, M., & Pamyatnykh, A. A. 1998, A&A, 332, 958
- Borkovits, T., & Hegedues, T. 1996, A&AS, 120, 63
- Catelan, M., & Smith, H. A. 2015, Pulsating Stars (Wiley-VCH), 2015,
- Conidis, G. J., & Delaney, P. A. 2013, PASP, 125, 639
- Cousins, A. W. J. 1976, MmRAS, 81, 25
- Dejaiffe, R. 2007, Ciel et Terre, 123, 122
- Fauvaud, S., Rodríguez, E., Zhou, A. Y., et al. 2006, A&A, 451, 999
- Fauvaud, S., Sareyan, J.-P., Ribas, I., et al. 2010, A&A, 515, A39
- Fu, J.-N., Zhang, C., Marak, K., et al. 2008, ChJA&A, 8, 237
- Giclas, H. L., Burnham, R., & Thomas, N. G. 1970, Lowell Observatory Bulletin, 7, 183
- Hintz, E. G., Joner, M. D., McNamara, D. H., et al. 1997, PASP, 109, 15 Q
- Kains, N., Arellano Ferro, A., Figuera Jaimes, R., et al. 2015, A&A, 578, A128
- Kim, C., & Sim, E.-J. 1999, Journal of Astronomy and Space Sciences, 16, 241
- Kim, C., Jeon, Y.-B., & Kim, S.-L. 2003, PASP, 115, 755
- Kopacki, G. 2013, AcA, 63, 91
- Lenz, P., & Breger, M. 2005, Communications in Asteroseismology, 146, 53
- Li, L.-J., & Qian, S.-B. 2010, AJ, 139, 2639
- Ma, S.-G., Esamdin, A., Ma, L., et al. 2018, Ap&SS, 363, #68
- Martinazzi, E., Kepler, S. O., Costa, J. E. S., et al. 2015, MNRAS, 449, 3535
- McNamara, D. H., & Feltz, K. A., Jr. 1978, PASP, 90, 275
- McNamara, D. 1997, PASP, 109, 1221
- McNamara, D. H. 2011, AJ, 142, 110
- Nemec, J., & Mateo, M. 1990, Confrontation Between Stellar Pulsation and Evolution, 11, 64
- Nemec, J. M., Balona, L. A., Murphy, S. J., Kinemuchi, K., & Jeon, Y.-B. 2017, MNRAS, 466, 1290
- Rodríguez, E., Rolland, A., & Lopez de Coca, P. 1990, Information Bulletin on Variable Stars, 3428, 1
- Rodríguez, E., & Breger, M. 2001, A&A, 366, 178

- Rodríguez, E., Fauvaud, S., Farrell, J. A., et al. 2007, *A&A*, 471, 255
- Sterken, C. 2005, *The Light-Time Effect in Astrophysics: Causes and cures of the O-C diagram*, 335, 3
- Song, F.-F., Esamdin, A., Ma, L., et al. 2016, *Research in Astronomy and Astrophysics*, 16, 154
- Tody, D. 1986, *Proc. SPIE*, 627, 733
- Tody, D. 1993, *Astronomical Data Analysis Software and Systems II*, 52, 173
- van Cauteren, P., & Wils, P. 2000, *Information Bulletin on Variable Stars*, 4872, 1
- Wolf, M., Crlikova, M., Basta, M., et al. 2002, *Information Bulletin on Variable Stars*, 5317, 1
- Yang, X. H., Fu, J. N., & Zha, Q. 2012, *AJ*, 144, 92
- Yang, T.-Z., Esamdin, A., Fu, J.-N., et al. 2018, *Research in Astronomy and Astrophysics*, 18, 002
- Zhou, A.-Y., Rodríguez, E., Jiang, S.-Y., Rolland, A., & Costa, V. 1999, *MNRAS*, 308, 631
- Zhou, A.-Y., Du, B.-T., Zhang, X.-B., & Zhang, R.-X. 2001, *Information Bulletin on Variable Stars*, 5061, 1